Review of Scientific Instruments

Ultrasonic waveguide based level measurement using flexural mode F(1,1) in addition to the fundamental modes

Cite as: Rev. Sci. Instrum. **90**, 045108 (2019); https://doi.org/10.1063/1.5054638
Submitted: 01 September 2018 . Accepted: 16 March 2019 . Published Online: 05 April 2019

Nishanth Raja, Krishnan Balasubramaniam, and Suresh Periyannan

Review of Scientific Instruments ARTICLE scitation.org/journal/rsi

Ultrasonic waveguide based level measurement using flexural mode F(1,1) in addition to the fundamental modes

Cite as: Rev. Sci. Instrum. 90, 045108 (2019); doi: 10.1063/1.5054638
Submitted: 1 September 2018 • Accepted: 16 March 2019 •
Published Online: 5 April 2019 • Corrected: 9 April 2019

Nishanth Raja,[a] Krishnan Balasubramaniam, and Suresh Periyannan[b]

AFFILIATIONS

Centre for Non-Destructive Evaluation, Department of Mechanical Engineering, Indian Institute of Technology Madras, Chennai 600036, India

[a]**Electronic mail:** nisanth.be@gmail.com.
[b]**Current address:** Department of Mechanical Engineering, National Institute of Technology Warangal, Warangal 506004, India.

ABSTRACT

This paper reports on an ultrasonic waveguide sensor for liquid level measurements using three guided wave modes simultaneously. The fundamental wave modes longitudinal L(0,1), torsional T(0,1), and flexural F(1,1) were simultaneously transmitted/received in a thin stainless steel wire-like waveguide using a standard shear wave transducer when oriented at an angle of 45° to the axis of the waveguide. Experiments were conducted in non-viscous fluid (water) and viscous fluid (castor oil). It was observed that the flexural F(1,1) wave mode showed a change in both time of flight (due to the change in velocity and dispersion effects) and amplitude (due to leakage) for different levels (0–9 cm) of immersion of the waveguide in a fluid medium. For the same level of immersion in the fluid, the L(0,1) and the T(0,1) modes show only a relatively smaller change in amplitude and no change in time of flight. The experimental results were validated using finite element model studies. The measured change in time of flight and/or the shift in central frequency of F(1,1) was related to the liquid level measurements. Multiple trials show repeatability with a maximum error of 2.5% in level measurement. Also, by monitoring all three wave modes simultaneously, a more versatile and redundancy in measurements of the fluid level inside critical enclosures of processing industries can be achieved by compensating for changes in the fluid temperature using one mode, while the level is measured using another. This ultrasonic waveguide technique will be helpful for remote measurements in physically inaccessible areas in hostile environments.

I. INTRODUCTION

The measurement of the liquid level in the processing and manufacturing industries (oil, petrochemical, etc.) is essential during process monitoring and custody transfer. Typically, in industries, two types of liquid level measurement techniques were reported,[1] namely, (a) invasive (contact type) and (b) non-invasive (non-contact type). In an invasive type of liquid level measurement concept, the sensor will be in contact with the liquid or embedded in it, for example, floats, dip probes, etc. The non-invasive techniques (acoustic sensors and ultrasonic and optical sensing methods) are widely used in specific applications which involve more safety requirements in the hazardous/inaccessible region of interest.[2] Different ultrasonic waveguide sensors (contact type) have been reported[3–10] for a wide range of applications, and also these sensors are capable of providing accurate measurements of the properties of the surrounding medium that includes temperature, fluid level, rheological properties, cure monitoring, etc.

In this work, we are interested in the development of a contact type waveguide sensor for the level measurement of viscous (castor oil) and non-viscous (water) fluids based on the changes in the behavior of L(0,1), T(0,1), and F(1,1) wave modes, using a single shear transducer. The transducer is rigidly fixed on the surface of the thin circular waveguide to simultaneously transmit/receive L(0,1), T(0,1), and F(1,1) wave modes in a pulse-echo modality. The three wave modes were explored for measurement of the level of fluids, and their sensitivity was examined.

Lynnworth *et al.*[11] had extensively reported on the fluid level, temperature, and flow of fluid measurement concepts using ultrasonic waveguide techniques. Later, different waveguide

TABLE I. Waveguide details.

Material	SS-308L
Mass density (ρ)–(kg/m^3)	7950
Young's modulus (E) (GPa)	183
Poisson's ratio (μ)	0.3
Waveguide diameter (D) (mm)	1

configurations were developed for fluid level sensing.[12–18] Initially, a rectangular ribbon like waveguide was used for level measurement.[12] Kim *et al.*[13] developed a waveguide of diamond-cross section for sensing the liquid's density, viscosity, and surface level using torsional modes in that waveguide. Spratt *et al.*[14] developed a torsional acoustic waveguide (circular waveguide with a rectangular sensing zone) sensor for measurement of the temperature and liquid level. Joo and Lee[15] described a plate waveguide sensor with a slit configuration for liquid level measurement at a hostile environment using the anti-symmetric A_0 mode. Subash and Balasubramaniam[16] proposed an ultrasonic guided wave system for liquid level sensing using the S_0 wave mode in a plate and the L(0,1) wave mode in a cylindrical rod. The parallel plate type waveguide was used for tank level measurement by Mann *et al.*[17] Recently, Liu *et al.*[18] demonstrated using a thin hollow wire for sensing the liquid level.

Most of the waveguide sensors have been developed based on the fundamental wave modes, i.e., either longitudinal L(0,1) or torsional T(0,1) mostly in cylindrical waveguides for fluid level sensing. Flexural wave modes inside a waveguide are expected to be more sensitive to fluid loading, as compared to the longitudinal and torsional wave modes, due to the relatively large out-of-plane displacement components, which lead to high rate of wave energy leakage from the waveguide surface into the fluid medium. Shin and Rose[19] presented the advantages of using flexural-guided waves in cylindrical structures for conditioning monitoring of pipelines. Knowles[20] studied the excitation and propagation of flexural waves to detect the surface level of an aerated fluid using the high-frequency pulse train technique. Pandey *et al.*[21] measured high-temperature properties of mold powder slags using the F(1,1) wave mode.

In this study, the objective is to develop an ultrasonic waveguide sensor for fluid level sensing using three fundamental wave modes [L(0,1), T(0,1), and F(1,1)] simultaneously. Here, the notations follow the L(x, y) or T(x, y) and F(x, y) format; the first integer (x) in the bracket corresponds to the circumferential order of the mode which specifies the variation of the mode shape around the circumference of the structure. The second integer (y) in the bracket indicates the mode number and differentiates the modes of the same family. Since

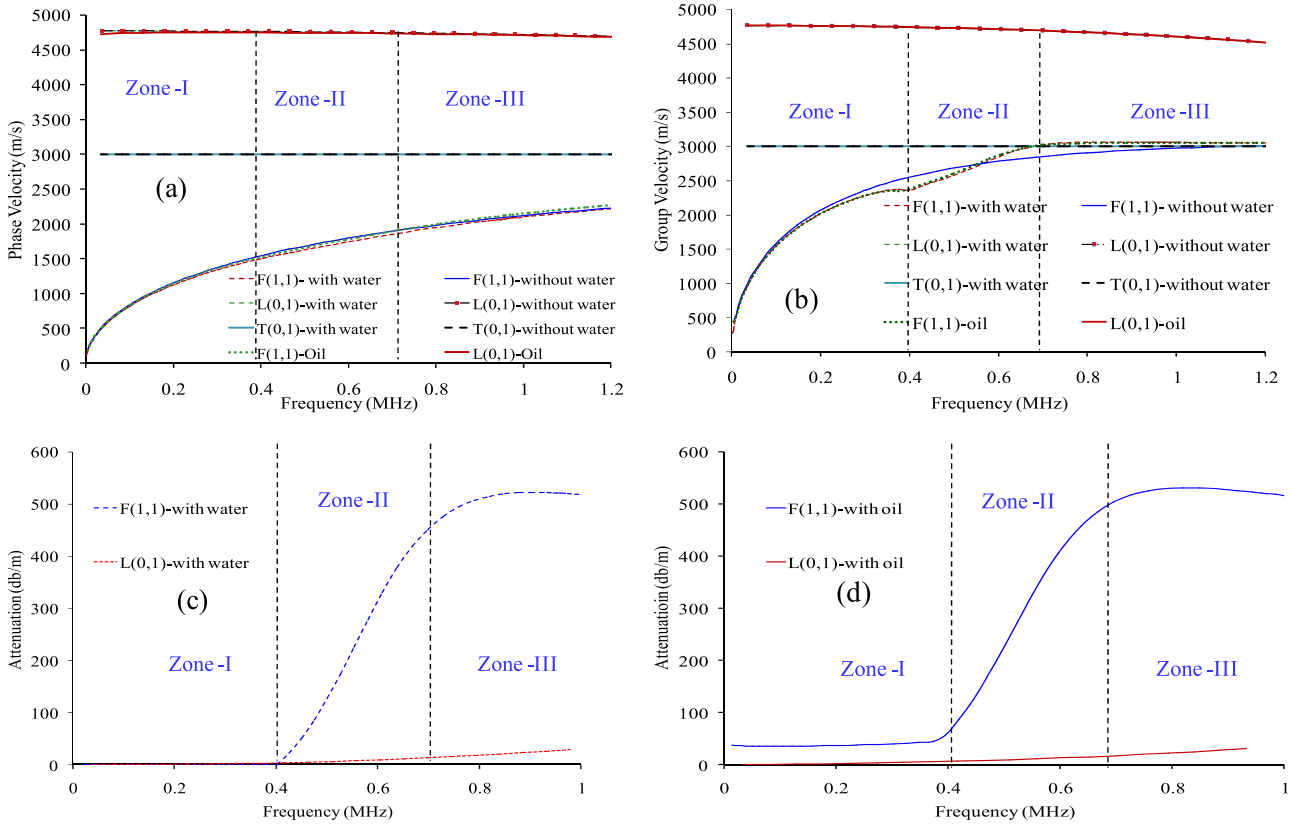

FIG. 1. Dispersion curves for stainless steel waveguide of 1 mm diameter: [(a) and (b)] phase velocity (Vp) and group velocity (Vg) of the waveguide at fluid loaded and free boundary conditions and [(c) and (d)] attenuation effects in water loaded and oil loaded conditions.

torsional and longitudinal waves are always axisymmetric, their first number in the bracket is always zero [L(0,1) and T(0,1) are symmetric wave mode, and F(1,1) is non-symmetric wave mode].[7] The wave mode excitation concepts in the cylindrical waveguide and their experimental results have been validated using commercially available finite element (FEM) package.

II. THE WAVEGUIDE SENSOR SETUP

A thin stainless steel (SS) waveguide was selected in this work. The waveguide dimensions and material properties are given in Table I, and the theoretically obtained dispersion curves and attenuation plot using Disperse software[22] are shown in Fig. 1, and their corresponding mode shapes are shown in Fig. 2. The particle displacements can reveal the characteristic behavior on the surface of the waveguide material that makes them useful for measuring the fluid properties. Here, F(1,1) mode shape shows that all three displacement components [axial (Uz), radial (Ur), and angular (Uq)] on the surface of the waveguide are maximum, which makes it sensitive toward the shear properties. In the case of L(0,1) mode, the axial displacement (Uz) is more dominant than the radial displacement (Ur) and can be used to measure the fluid properties such as density and bulk modulus. Similarly, T(0,1) mode shape shows displacements in the angular direction only and it is suitable for measurement of the shear properties of the fluid.

An operational frequency of 500 kHz was preferred in this work in order to limit the level of dispersion [Fig. 1 (zone-II)]. A conventional shear transducer with a bandwidth of 250 kHz–620 kHz was coupled to the waveguide using a very thin layer of viscous silicone based ultrasonic couplant and constant pressure on the surface of the waveguide. The transducer was oriented at an angle of 45° to the axis of the cylindrical waveguide, as shown in Fig. 3(a) for simultaneous transmission/reception of L(0,1), T(0,1),[23,24] and F(1,1) wave modes, and the obtained A-scan signal is shown in Fig. 3(b). The earlier reported experimental setup[24–26] was used for acquiring these wave modes in the thin cylindrical waveguide.

By adjustment of the normal force between the transducer surface and the waveguide, it was feasible to control the relative amplitudes of the three modes. It was determined that at an optimal force, obtained through trial-and-error mode, the F(1,1) wave mode was found to be maximum and this condition was used for all experiments reported here. Figures 1(a) and 1(b) show that the F(1,1) mode is relatively more dispersive compared to the T(0,1) and L(0,1) modes in the range of frequencies considered here, i.e., 450–550 kHz (zone-II). The F(1,1) mode leakage (attenuation) due to fluid loading (oil and water) is relatively higher when compared to the

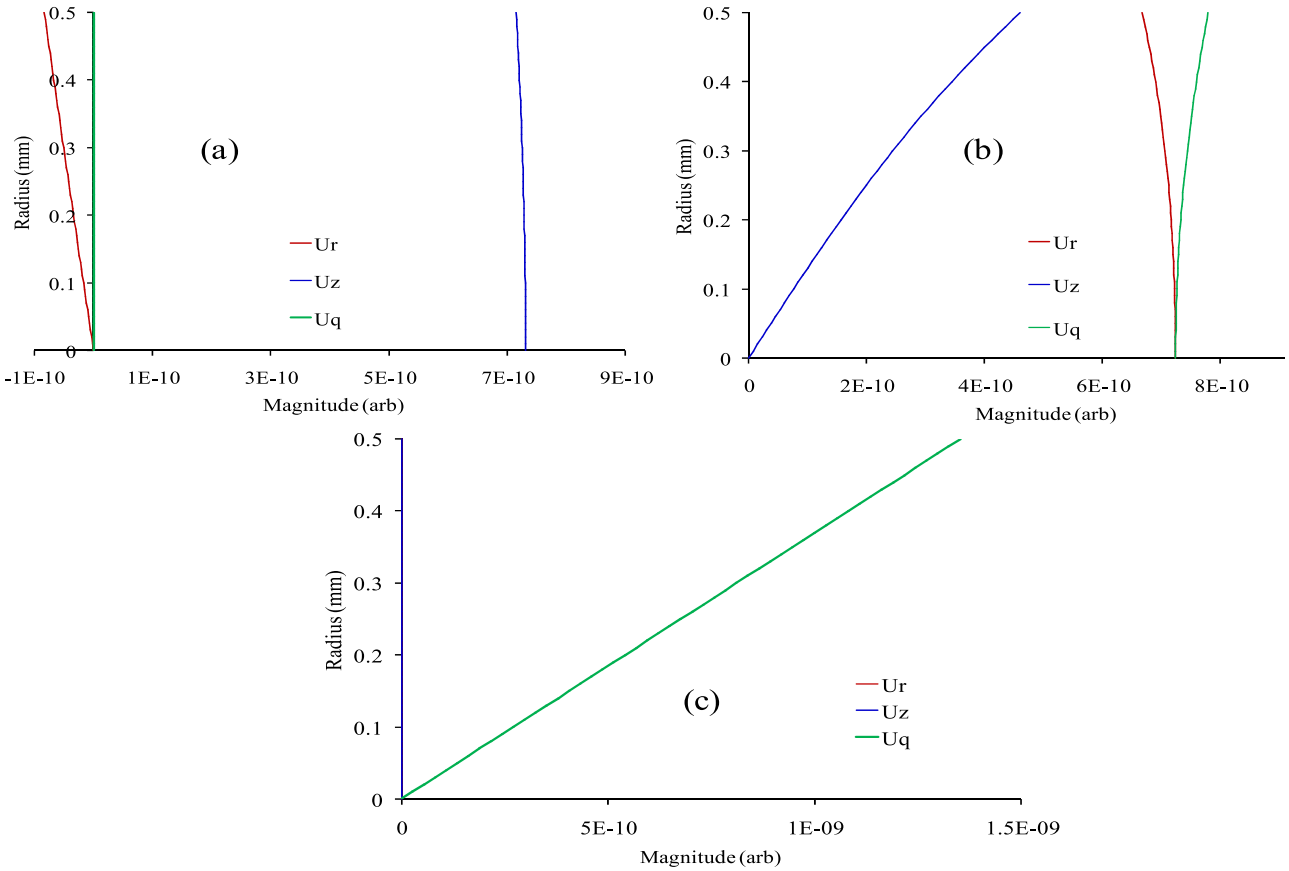

FIG. 2. Mode shapes for (a) L(0,1), (b) F(1,1), and (c) T(0,1) modes in a stainless steel wire of diameter 1 mm at frequency 500 kHz.

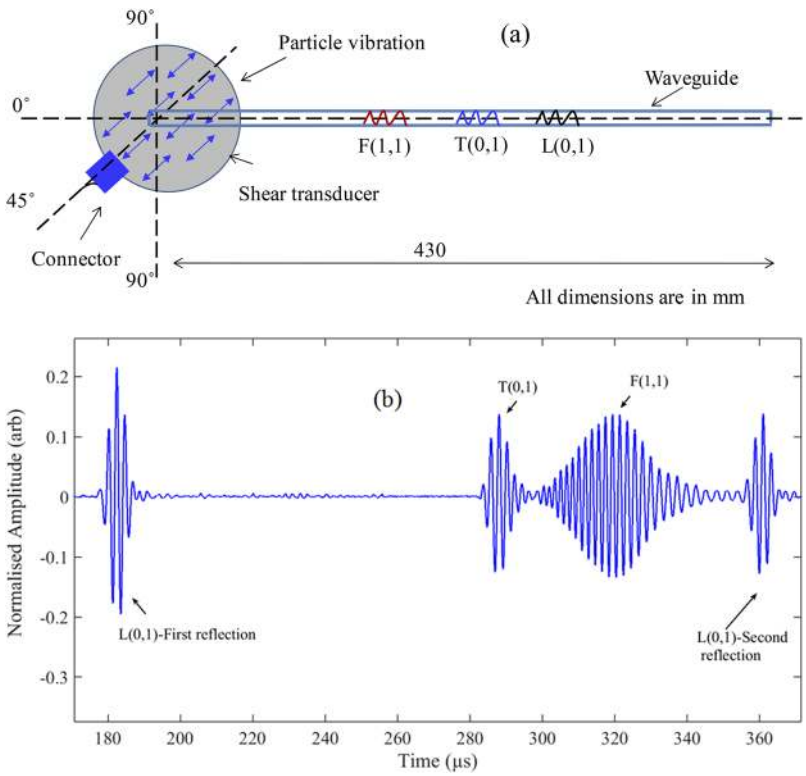

FIG. 3. (a) Shows the orientation (45°) between the waveguide and shear transducer and (b) L(0,1), T(0,1), and F(1,1) wave mode reflected signals observed experimentally from the waveguide (in air medium).

torsional and longitudinal modes, as shown in Figs. 1(c) and 1(d), also explained elsewhere.[22,27] In addition, it may be noted that below 400 kHz, the leakage to the surrounding fluid is negligible and hence the attenuation values are also insignificant.

In order to understand the F(1,1) wave mode behavior at different fluid loading conditions, level measurement experiments were carried out from 0 to 9 cm on both oil (viscous fluid) and water (non-viscous fluid), and the detailed FEM and experimental observations on this insight will be explained in the Secs. III and IV.

III. FEM SIMULATION STUDIES

FEM study was conducted using the commercial package ABAQUS® 6.12[28] to analyze the simultaneous generation and reception of the three wave modes [L(0,1), T(0,1), and F(1,1)] and their behavior in a straight waveguide that is embedded in air and in water (at different levels of immersion). The waveguide dimensions, material properties, and FEM parameters are shown in Tables I and II. A Hanning input pulse (5 cycles) with a center frequency of 500 kHz with a maximum displacement of 1×10^{-6} m was applied on the surface of the thin SS ultrasonic waveguide, as shown in Fig. 3(a). The reflected signals were received near the transduction region of the waveguide. The FEM results in Fig. 4(a) show the absolute displacements for the wave modes generated, and Fig. 4(b) confirms the simultaneous excitation/reception of all three wave modes. However, for comparing the FEM with the experiments, the plots have been represented by normalizing to the maximum absolute displacement amplitude value. Furthermore, the FEM approach was extended to study the behavior of these wave modes, while the waveguide was embedded in the water medium at different levels. The obtained A-scan signals were analyzed based on the reflected signal attenuation due to wave leakage from the waveguide to the surrounding medium (water).

The rate of wave leakage was observed from all three wave modes in different levels of the fluid medium. Finally, from the obtained A-scan signals, as shown in Fig. 4(b), more sensitivity was observed from the flexural wave mode F(1,1) as compared to L(0,1) and T(0,1) wave modes due to attenuation and dispersion effects, i.e., a significant change in amplitude as well as a change in time of flight (δTOF) were observed. Based on this FEM study, the waveguide sensor was employed in different fluid media for level measurement experiments.

Additionally, in this FEM study, the F(1,1) mode was then confirmed using frequency-wavenumber analysis for wave mode

TABLE II. FEM parameters.

Element size criteria	(λ/48)
Element type	8 node hexahedral
Frequency (f) (kHz)	500
No. of cycles	5
Material	SS-308L
Mass density (ρ) (kg/m^3)	7950
Young's modulus (E) (GPa)	183
Poisson's ratio (μ)	0.3

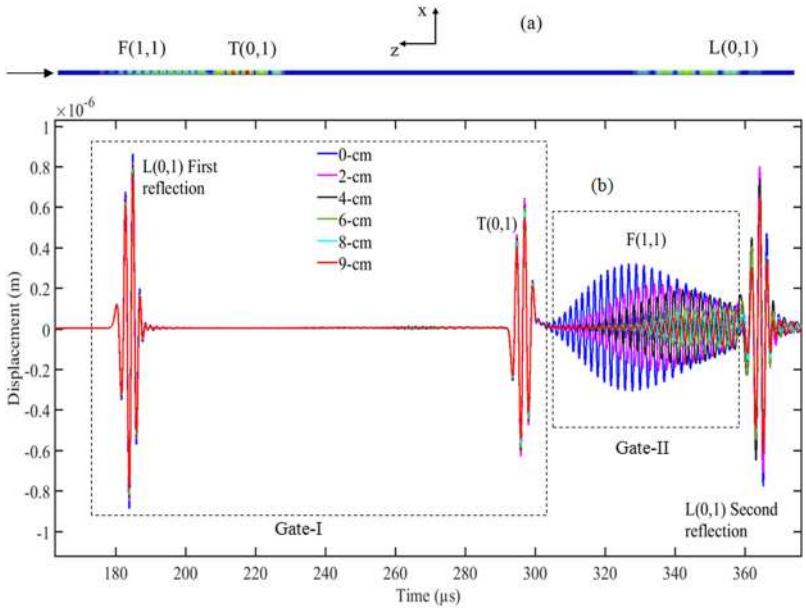

FIG. 4. (a) Snapshot of the FEM model for simultaneous generation of all three wave modes and (b) A-scan signal as obtained from simulations for different fluid levels for L(0,1) T(0,1), and F(1,1) mode propagation.

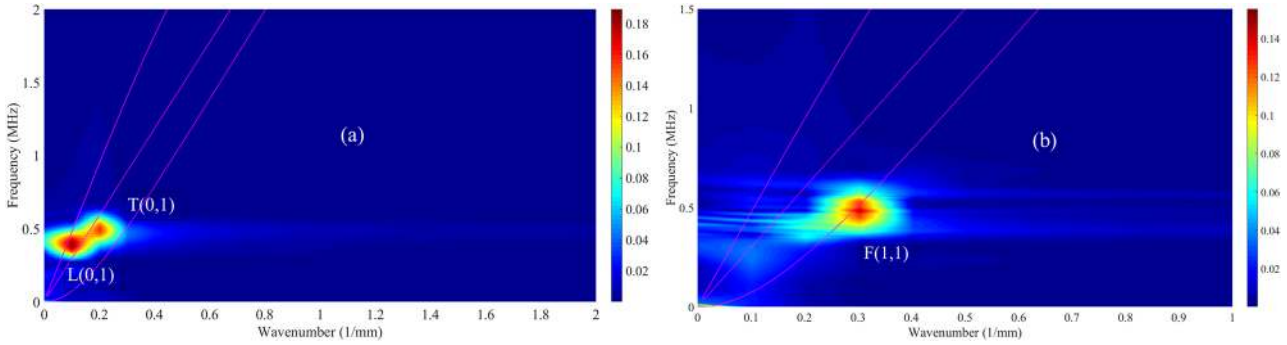

FIG. 5. The 2D FFT overlaid with dispersion curves for identification of (a) L(0,1) and T(0,1) from gate I [Fig. 4(b)] and (b) F(1,1) wave mode from gate II [Fig. 4(b)].

identification and wave propagation analysis[29] at the corresponding diameter of the wire waveguide. This used the displacements at each node on the surface of the waveguide and using a 2D-FFT (fast Fourier transform) inversion, and the time-frequency plots were obtained, as shown in Figs. 5(a) and 5(b), by time gating the individual signals [Fig. 4, gate-I L(0,1) and T(0,1), gate-II F(1,1)]. The time-frequency representation in this figure, overlapped with the dispersion curves, clearly indicate the presence of three modes in the signal, i.e., L(0,1), T(0,1), and F(1,1), respectively.[30]

IV. EXPERIMENTAL SETUP AND PROCEDURE FOR LEVEL MEASUREMENT EXPERIMENTS

The schematic of the experimental setup is shown in Fig. 6. The waveguide was positioned vertically in the container for level measurement experiments. The reference level scale with a range of 0–10 cm and division of 1 mm was marked on the test beaker. One end of the waveguide was connected to the shear transducer, and the other end of the waveguide was immersed inside the liquid for level

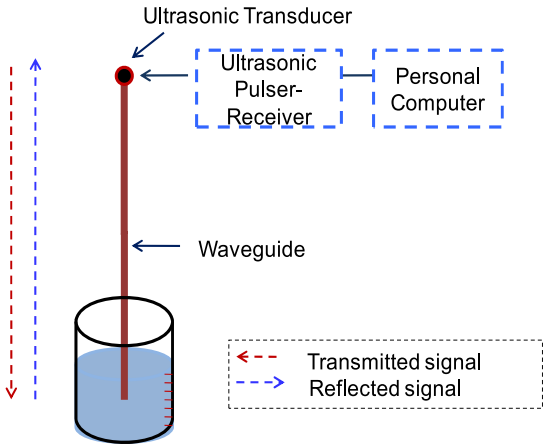

FIG. 6. Schematic of the experimental setup for liquid level measurement using a single waveguide.

measurement. The surface of the waveguide was rigidly fixed to the shear transducer (Panametrics V151—500 kHz) for simultaneously transmitting/receiving all three wave modes in the thin waveguide using an ultrasonic pulser/receiver (TechnoFour UTUSB2.0) with 100 MHz sampling rate. The level sensing experiments were carried out in two different fluids (a) water and (b) castor oil which are non-viscous and viscous, respectively.

V. RESULTS AND DISCUSSION

The liquid level sensing was based on the measurement of ultrasonic wave behavior in the straight waveguide configuration. The initial A-scan signal was obtained when the waveguide was not subjected to fluid loading (air medium, i.e., 0-cm), as shown in Fig. 7, and subsequently, the fluid (water) was filled gently in the cylindrical container with an increment of 10 mm. The A-scan signals were acquired at each 10 mm interval while filling 90 mm depth of water in the beaker, and the acquired corresponding A-scan signals are shown in Fig. 7.

Here, a significant change in amplitude was observed for all three wave modes [L(0,1), T(0,1), and F(1,1)]; also a significant change in time of flight (δTOF) of the F(1,1) signal was observed at every 10 mm increment of fluid loading. The water level was measured by monitoring the change in amplitude as well as the change in time of flight (δTOF) from the obtained A-scan signals. Experiments were repeated for few trials, and it was observed that when the sensor was exposed to different water levels, the sensitivity of the peak amplitude feature was significantly higher in the flexural wave mode F(1,1) as compared to the other two wave modes [L(0,1) and T(0,1)]. This confirms the results of the attenuation of F(1,1), as shown in Fig. 1(c). The time of flight of the F(1,1) mode was also found to be sensitive to the fluid level, indicating that the group velocity of the F(1,1) mode has a high dependency on the fluid level, while the other modes did not indicate any measurable change in the time of flight.

While monitoring the signals for the F(1,1) modes, it was very critical to extract the change in time-of-flight (δTOF) and peak amplitude information from the A-scan signals using the peak

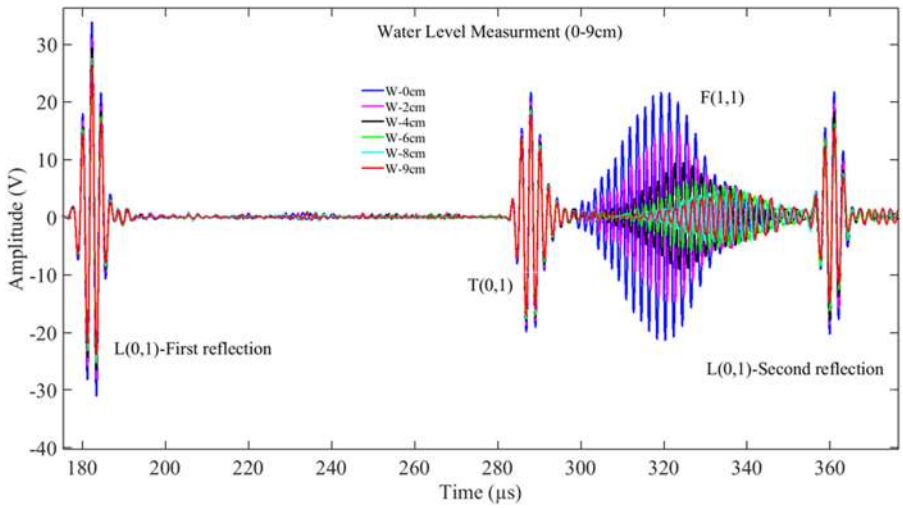

FIG. 7. Reflected L(0,1), T(0,1), and F(1,1) modes in the A-scan signals observed at different fluid levels.

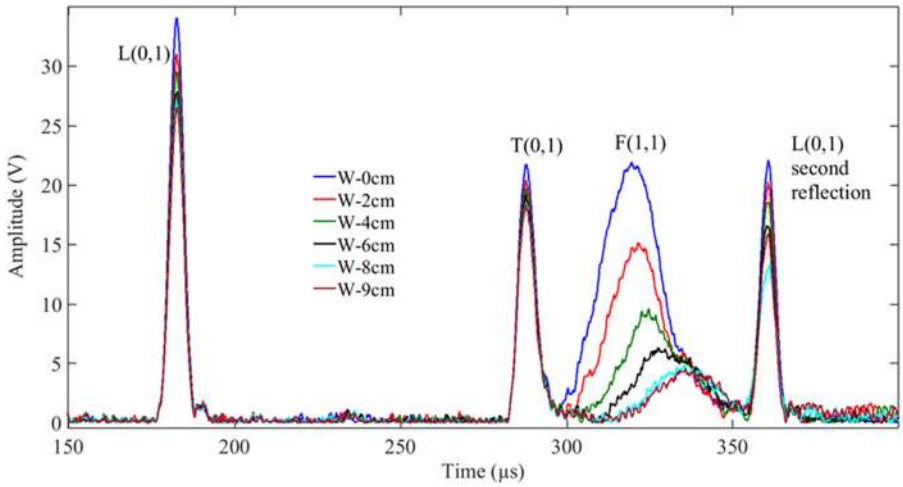

FIG. 8. The Hilbert transform of the reflected L(0,1), T(0,1) and F(1,1) modes observed at different fluid levels.

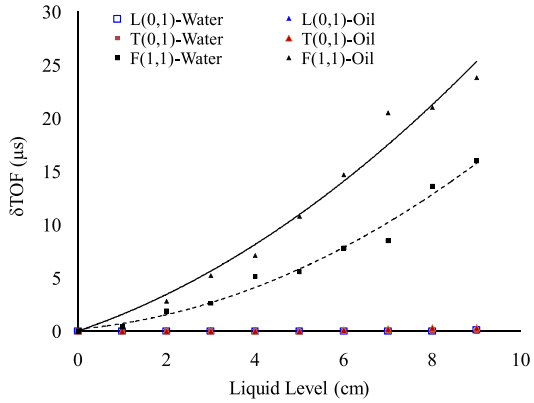

FIG. 9. Illustrates the change in time of flight (δTOF) of the L(0,1), T(0,1), and F(1,1) wave modes at different fluid levels.

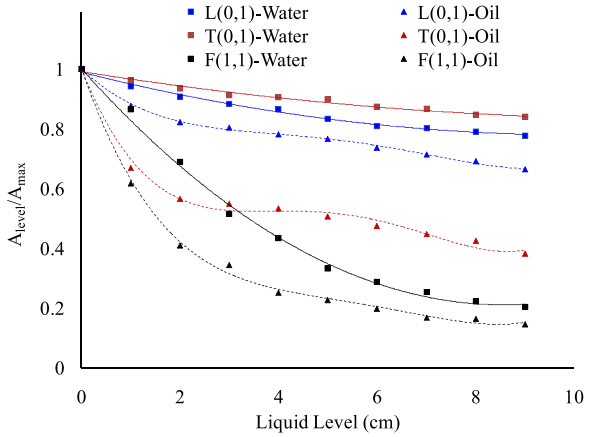

FIG. 10. Normalized amplitude of L(0,1), T(0,1), and F(1,1) wave modes at different fluid levels.

tracking concept.[24–26] Hence, the Hilbert transform was identified as an appropriate tool and utilized for monitoring the signal to measure the δTOF (by tracking the change in the peak value) and peak amplitude shifts during level measurements, as shown in Fig. 8.

The δTOF effect on all three wave modes is illustrated in Fig. 9, when the sensor was immersed in different levels of water and castor oil. The following observations were made:

- When the waveguide was embedded in a non-viscous fluid, a negligible change in TOF (less than 1%) was observed in L(0,1) and T(0,1) wave modes, whereas significant changes were observed in F(1,1) due to the dispersion and attenuation effects
- The attenuation of the F(1,1) wave mode was higher in the viscous fluid, and more change in TOF was observed as compared to δTOF changes in water.

Since substantial changes were observed in the F(1,1) wave mode from the viscous and non-viscous liquids during level measurement experiments, the single calibration curve based on the change in time of flight (δTOF) of the F(1,1) wave mode at different levels will be adequate for liquid level measurement.

The 2nd order polynomial fit was found to be optimum and used to obtain the calibration equations of the F(1,1) wave mode for non-viscous fluid at different liquid levels. The 2nd order polynomial fit was found to be optimum and used to obtain the calibration equations of the F(1,1) wave mode for viscous and non-viscous fluids at different liquid levels. The obtained calibration equations are shown in Table III, where "x" and "y" represent the level in cm and the change in the time of flight (δTOF) value, respectively.

TABLE III. Second-order polynomial fit coefficients for δTOF vs liquid level of F(1,1).

Second-order polynomial equation for level measurement
$y = ax^2 + bx + c$

F(1,1)	a	b	c	R^2
δTOF—water	0.117	1.409	0.010	0.979
δTOF—oil	0.150	0.444	0.010	0.981

Additionally, the signal normalized amplitude (A_{level}/A_{max}) of reflected signals of all three wave modes was tracked at each interval and is shown in Fig. 10. Here, A_{max} is the amplitude of the end reflected signal with no fluid loading and A_{level} is the peak amplitude when the sensor is immersed in different levels. The normalized amplitude (A_{level}/A_{max}) of reflected signals of all three wave modes was tracked at each interval of fluid loading levels for both water and oil and is shown in Fig. 10. From the obtained results, the following observations were made:

- During the water level measurement experiments, the change in amplitude of the L(0,1) wave mode is relatively higher as compared to the T(0,1) mode. Nevertheless, during the oil level measurement experiments, a substantial drop in amplitude of the T(0,1) wave mode was observed as compared to the L(0,1) mode.

TABLE IV. (a) Second-order polynomial fit coefficients for the change in amplitude on water level measurement. (b) Second-order polynomial fit coefficients for the change in amplitude on oil level measurement.

Fluid medium (water): second-order polynomial equation
$y = ax^2 + bx + c$

Wave mode	a	b	c	R^2
L(0,1)	0.002	−0.042	0.990	0.992
T(0,1)	0.001	−0.026	0.991	0.981
F(1,1)	0.011	−0.190	1.015	0.996

Fluid medium (oil): fourth-order polynomial equation
$y = ax^4 + bx^3 + cx^2 + dx + e$

Wave mode	a	b	c	d	e	R^2
L(0,1)	0.001	−0.006	0.044	−0.155	1.00	0.99
T(0,1)	0.001	−0.018	0.133	−0.419	1.00	0.99
F(1,1)	0.002	−0.013	0.118	−0.475	1.00	0.99

- As predicted in the FEM model, extensive changes were observed in the peak amplitude of the F(1,1) mode due to fluid loading by both water and oil. As anticipated, the drop in amplitude due to surface loading of oil was relatively higher in F(1,1) compared to the other two modes [L(0,1) and T(0,1)].

From the obtained results, it is evident that the higher the waveguide immersion in the fluid media (water and oil), the more the attenuation of received signal amplitude. Hence, significant changes in signal amplitude were observed in the L(0,1), T(0,1), and F(1,1) wave modes during level measurement experiments for viscous and non-viscous liquids.

In order to obtain the amplitude based calibration equation for the non-viscous fluid, an second order polynomial fit was found to be optimum and the obtained polynomial fit coefficients for L(0,1), T(0,1), and F(1,1) wave modes are shown in Table IV. Similarly, for the viscous fluid, fourth order polynomial fit was found to be optimum and the obtained calibration equations are shown in Table IV where "x" and "y" represent the level in cm and the normalized amplitude value, respectively.

Subsequently, the individual modes were extracted in the time domain using time gates and after applying the zero-padding (in order to keep the record lengths similar), the frequency spectrums are plotted in Figs. 11(a)–11(c). The change in the peak amplitude of the peak frequency was monitored for all three wave modes and is plotted in Fig. 11(d). The change in peak frequency was found to be a predominant effect for the F(1,1) reflected signal at each level of waveguide immersion. The change in peak amplitude was monitored for all three wave modes [L(0,1), T(0,1), and F(1,1)] at every 10 mm increment of fluid loading and is plotted in Fig. 11(d). The peak frequency of F(1,1) at each level of waveguide immersion for viscous and non-viscous fluid was correlated to the attention of the F(1,1) wave mode and is shown in Fig. 12. These frequency domain measurements are expected to be an improved feature for measuring the level of fluid when compared to the time domain.

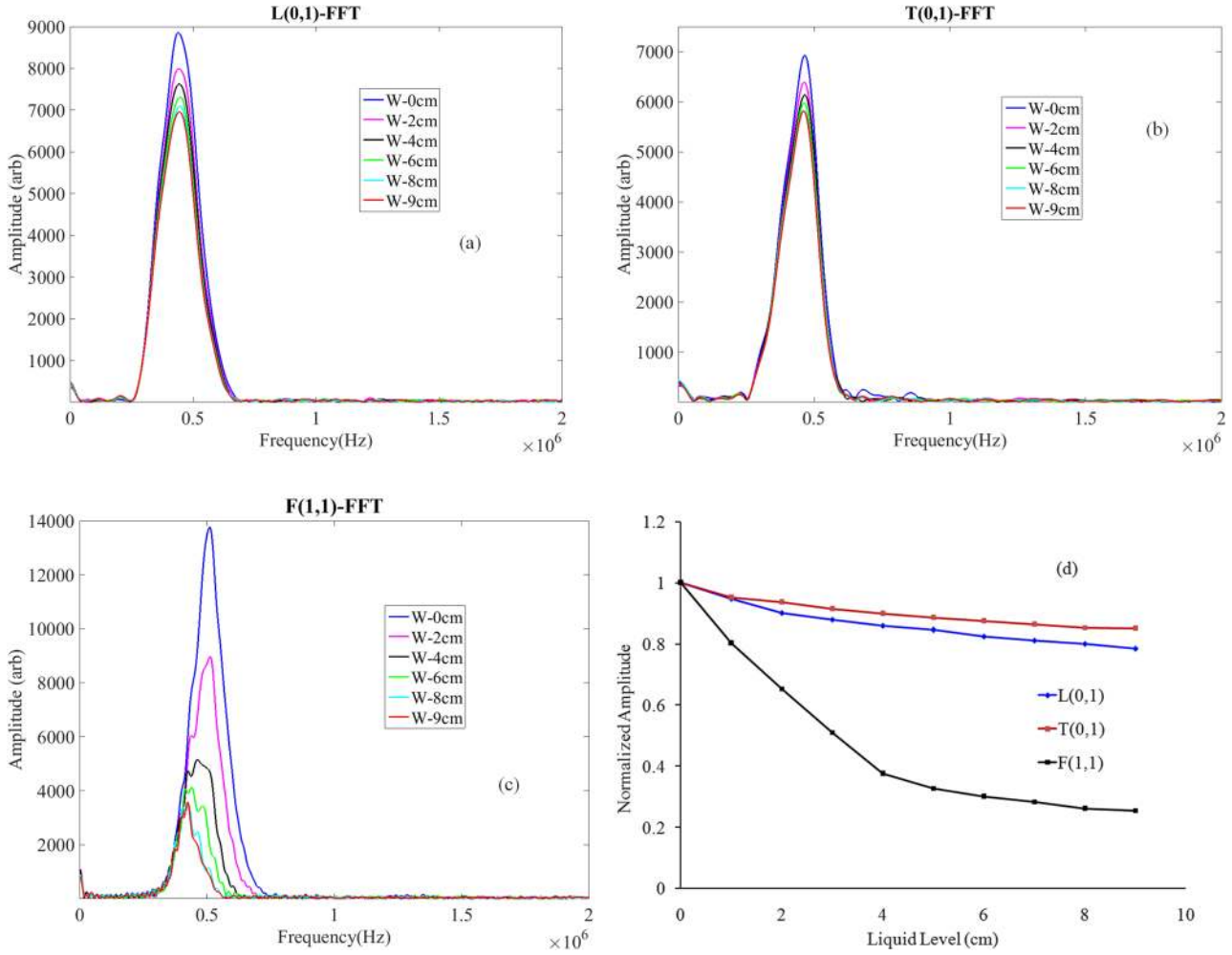

FIG. 11. Frequency response of the guided wave modes (a) L(0,1), (b) T(0,1), and (c) F(1,1) at different fluid levels and (d) comparison of shift in peak frequency amplitudes vs fluid levels.

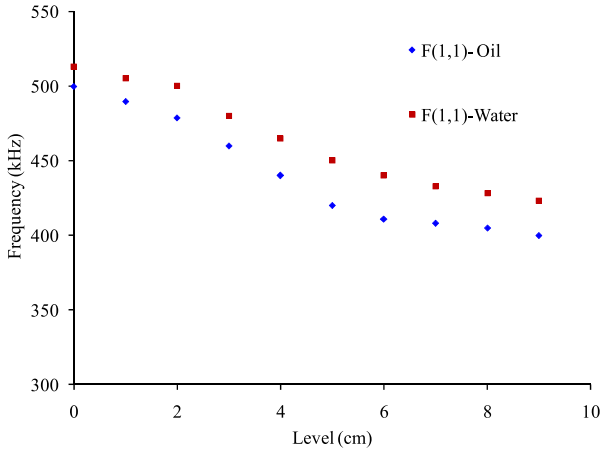

FIG. 12. Peak frequency shift of the F(1,1) wave mode at different fluid levels in water and oil loaded conditions.

From the obtained results, it was observed that the flexural wave mode F(1,1) showed significantly higher sensitivity to the surrounding fluid as compared to the other two guided wave modes. Here, for the water fluid loaded condition of 9 cm (i.e., travel of 18 cm), the change in the peak frequency of the frequency spectrum between the un-loaded (f = 500 kHz) and the fluid loaded condition (f = 425 kHz) is approximately 75 kHz. Since the F(1,1) mode is dispersive in this region, the corresponding change in group velocity from Fig. 1(b) [i.e., Vg at 500 kHz (0 cm) is 2700 m/s and Vg at 420 kHz (9 cm) is 2300 m/s] is approximately 300 m/s. The corresponding change in ToF between the unloaded and loaded conditions can be calculated to be approximately 14 μs which is in the same order as measured and observed in both experiments and the FEM model. Along the same lines, the attenuation (α) changes with depth of immersion, as seen from Fig. 1(c), from α (500 kHz for 0 cm) = 137 dB/m to α (420 kHz for 9 cm) = 22 dB/m. Hence, the attenuation as measured and predicted by the model for the 9 cm case is comparable to the 22 dB/m case calculated here. The compiled calibration equation for the F(1,1) wave mode with respect to changes in amplitude drop, frequency shift, and δTOF of the signal for water is shown in Table V where x and y represent the liquid level and change in amplitude, frequency, and δTOF.

In addition to the fluid level information, this waveguide sensor system has a great potential to measure several parameters related to acoustic properties of the surrounding fluid, such as the viscosity and density of the fluid. However, due to the high sensitivity and dispersive nature, the flexural wave mode is more suitable for precise level measurement and useful for short-range fluid level measurement (i.e., less than 10 cm), whereas the L(0,1) and T(0,1) wave modes show reduced sensitivity and hence can be utilized for very long range liquid level measurement (i.e., more than 10 cm).

TABLE V. Second-order polynomial fit coefficients for water level measurements.

The second-order polynomial equation for water level measurement

$$y = ax^2 + bx + c$$

F(1,1)Wave mode	a	b	c	R^2
δTOF	0.117	1.409	0.010	0.979
Change in amplitude	0.011	−0.190	1.015	0.996
Change in frequency	0.56	−16.35	521.57	0.98

VI. REPEATABILITY EXPERIMENTS

Multiple trials were conducted to validate the repeatability of this technique. The level measurement experiments were repeated for non-viscous fluid and the obtained shift in peak frequency and δTOF at different fluid levels of F(1,1) are shown in Figs. 13 and 14. From the figures it is evident that the data were found to be consistent and conform to be repeatable with an error percentage

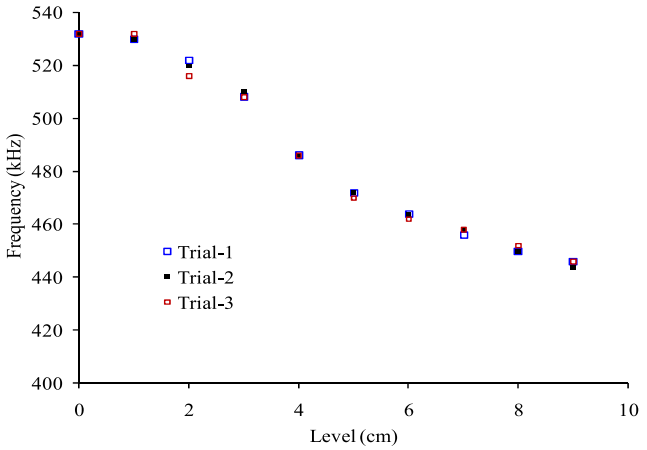

FIG. 13. Peak frequency shift of the F(1,1) wave mode at different fluid levels for different trials.

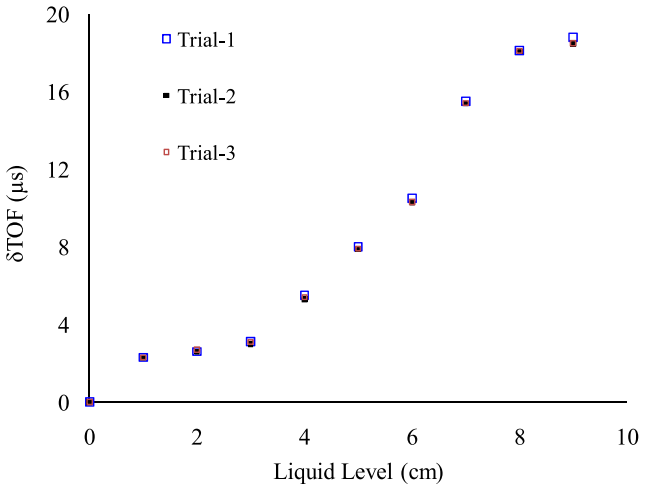

FIG. 14. Change in time of flight (δTOF) of the F(1,1) wave modes at different fluid levels.

less than 2.5%. Also, a different transducer with a center frequency of 525 kHz was selected for this repeatability experiment and the obtained results follow the same pattern of the previous transducer. The time corresponding to the signal peak becomes delayed to a certain degree, which is a result of the decrease in wave velocity due to the shift in the peak frequency. Combined with a calibrated curve of the δTOF and shift in the peak frequency against the liquid level, monitoring the rapid changes in fluid level will be possible.

VII. CONCLUSIONS

In this work, we reported a novel concept for measuring the level of fluids using an ultrasonic guided wave technique. Here, all three wave modes [L(0,1), T(0,1), and F(1,1)] were simultaneously transmitted/received in a thin stainless steel (SS) waveguide using a single shear transducer.

The actual experimental condition was replicated in the FEM studies for validating the level measurement experiments. Also, in this study, the dispersive effects were observed for all three wave modes [L(0,1), T(0,1), and F(1,1)] at different fluid levels. The obtained FEM results and experimental results were well in agreement in this level sensor design for level sensing in different fluid media.

The liquid level can be measured based on the significant changes in the amplitude drop, frequency shift, and time shift when the waveguide was embedded in the fluid at different levels. In the same operating frequency, more sensitivity was observed in the flexural wave F(1,1) mode as compared to the other two wave modes. In summary, the proposed waveguide sensor is very robust and can adapt to complex industrial environments for more versatile and redundant measurements of the fluid level in critical enclosures. However, the operating frequency of the flexural mode must be chosen appropriately using the attenuation curve for level measurement experiments. This will be dependent on the material and diameter of the circular waveguide. Other cross-sectional geometries can also be explored in future studies for understanding the behavior of F(1,1) modes on different waveguide configurations.

REFERENCES

[1] *The Engineer's Guide to Level Measurement* (Emerson Process Management, 2013); available at https://go.emersonautomation.com/rmt-en-l-level-resources?utm_source=rmt_us-elql-hbook_arop&utm_medium=mixe&utm_content=lre_guides&utm_campaign=19grmtl-lvel_resources_eg83.

[2] H. K. Singh, S. K. Chakraborty, H. Talukdar, N. M. Singh, and T. Bezboruah, IEEE Sens. J. **11**, 391 (2011).

[3] S. Periyannan, P. Rajagopal, and K. Balasubramaniam, AIP Adv. **6**(6), 065116 (2016).

[4] W. Voss, "Ultrasonic filling level sensor," U.S. patent No. 7,168,314 (30 January 2007).

[5] N. Raja, K. Balasubramaniam, and S. Periyannan, IEEE Sens. J. **18**(14), 5699 (2018).

[6] R. Kazys, L. Mazeika, R. Sliteris, and R. Raisutis, Ultrasonics **54**(4), 1104 (2014).

[7] M. G. Silk and K. F. Bainton, Ultrasonics **17**(1), 11–19 (1979).

[8] V. S. K. Prasad, K. Balasubramaniam, E. Kannan, and K. L. Geisinger, J. Mater. Process. Technol. **207**, 315 (2008).

[9] T. Vogt, M. Lowe, and P. Cawley, J. Acoust. Soc. Am. **114**(3), 1303 (2003).

[10] H. H. Bau, J. O. Kim, L. C. Lynnworth, and T. H. Nguyen, U.S. patent 4,893,496 (16 January 1990).

[11] L. C. Lynnworth, *Ultrasonic Measurements for Process Control: Theory, Techniques, Applications* (Academic Press, 2013).

[12] S. C. Rogers and G. N. Miller, IEEE Trans. Nucl. Sci. **29**(1), 665 (1982).

[13] J. O. Kim, H. H. Bau, Y. Liu, L. C. Lynnworth, S. A. Lynnworth, K. A. Hall, and J. A. Korba, IEEE Trans. Ultrason., Ferroelectr., Freq. Control **40**(5), 563 (1993).

[14] W. K. Spratt, J. F. Vetelino, and L. C. Lynnworth, in *Ultrasonics Symposium (IUS)* (IEEE, 2010), p. 702.

[15] Y.-S. Joo and J.-H. Lee, in *Transactions of the Korean Nuclear Society Spring Meeting* (Korean Nuclear Society, 2006), p. 25.

[16] N. N. Subhash and K. Balasubramaniam, Insight-Non-Destr. Test. Cond. Monit. **56**(11), 607 (2014).

[17] S. Mann, S. Lindner, F. Barbon, S. Linz, A. Talai, R. Weigel, and A. Koelpin, in *IEEE Topical Conference* (IEEE, 2014), p. 4.

[18] B. Liu, D. Y. Wang, and A. Wang, IEEE Sens. J. **16**, 2317 (2015).

[19] H. J. Shin and J. L. Rose, Ultrasonics **37**, 355 (1999).

[20] T. J. Knowles, "Acoustic flexural order level sensor," U.S. patent 9,285,261 (15 March 2016).

[21] J. C. Pandey, M. Raj, S. N. Lenka, P. Suresh, and K. Balasubramaniam, Ironmaking Steelmaking **38**(1), 74 (2011).

[22] B. N. Pavlakovic, M. J. S. Lowe, P. Cawley, and D. N. Alleyne, Rev. Prog. Quant. Nondestr. Eval. **16**, 185 (1997).

[23] S. Periyannan and K. Balasubramaniam, Rev. Sci. Instrum. **86**(11), 114903 (2015).

[24] K. Balasubramaniam and S. Periyannan, "Waveguide technique for the simultaneous measurement of temperature dependent properties of materials," U.S. patent 20,160,153,938 (2 June 2016).

[25] S. Periyannan and K. Balasubramaniam, Exp. Mech. **56**, 1257 (2016).

[26] R. Nishanth, K. Lingadurai, S. Periyannan, and K. Balasubramaniam, Insight-Non-Destr. Test. Cond. Monit. **59**(7), 358 (2017).

[27] Z. Fan, M. J. S. Lowe, M. Castaings, and C. Bacon, J. Acoust. Soc. Am. **124**(4), 2002 (2008).

[28] D. Hibbitt, B. Karlsson, and P. Sorensen, *Abaqus 6.12 Documentation and User Manual* (Dassault Systems Simulia Corp, 2012).

[29] D. N. Alleyne and P. Cawley, J. Acoust. Soc. Am. **89**, 1159 (1991).

[30] Z. Tian and L. Yu, J. Intell. Mater. Syst. Struct. **25**, 1107 (2014).